

Article

Integrated Risk Assessment of Waterlogging in Guangzhou Based on Runoff Modeling, AHP, GIS and Scenario Analysis

Shuai Xie ^{1,2}, Wan Liu ^{1,2}, Zhe Yuan ^{1,2,*}, Hongyun Zhang ³, Hang Lin ^{1,2} and Yongqiang Wang ^{1,2}

¹ Changjiang River Scientific Research Institute of Changjiang Water Resources Commission, Wuhan 430010, China

² Hubei Provincial Key Laboratory of Basin Water Resources and Ecological Environment, Wuhan 430010, China

³ Anhui Provincial Traffic Survey and Design Institute Co., Ltd., Hefei 230011, China

* Correspondence: yuanzhe@mail.crsri.cn; Tel.: +86-13716565927

Abstract: Among the various natural disasters encountered by cities, rainstorm waterlogging has become a serious disaster, affecting the sustainable development of cities. Taking Guangzhou as the research object, based on disaster system theory and risk triangle theory, the evaluation framework “risk of hazard causing factors—sensitivity of disaster environment—vulnerability of hazard bearing body” was selected to construct the waterlogging risk assessment model of Guangzhou. The weighted comprehensive evaluation method (AHP) was used to determine the index weight, and the rainfall runoff inundation range under different rainstorm scenarios was deduced through a Soil Conservation Service (SCS) runoff generation model and GIS local equal volume passive inundation simulation. The results show that when the precipitation in 2 h is less than 100 mm, the inundation range increases by 3.4 km² for every 10 mm increase in precipitation; When the precipitation in 2 h is greater than 100 mm, the inundation range will increase by 18 km² for every 10 mm increase in precipitation. The total area of medium and high flood risk in Guangzhou is 441.3 km², mainly concentrated in Yuexiu District, Liwan District, Haizhu District and Tianhe District.

Keywords: waterlogging risk assessment; SCS runoff generation model; volumetric method; Guangzhou



Citation: Xie, S.; Liu, W.; Yuan, Z.; Zhang, H.; Lin, H.; Wang, Y. Integrated Risk Assessment of Waterlogging in Guangzhou Based on Runoff Modeling, AHP, GIS and Scenario Analysis. *Water* **2022**, *14*, 2899. <https://doi.org/10.3390/w14182899>

Academic Editor: Wei Sun

Received: 26 July 2022

Accepted: 14 September 2022

Published: 16 September 2022

Publisher's Note: MDPI stays neutral with regard to jurisdictional claims in published maps and institutional affiliations.



Copyright: © 2022 by the authors. Licensee MDPI, Basel, Switzerland. This article is an open access article distributed under the terms and conditions of the Creative Commons Attribution (CC BY) license (<https://creativecommons.org/licenses/by/4.0/>).

1. Introduction

In recent years, extreme weather phenomena have become prominent, and the intensity and frequency of urban rainstorms are also increasing [1]. With the rapid urbanization process in China, urban waterlogging disasters caused by heavy rainfall have become increasingly frequent, bringing great losses to major cities [2–4]. The heavy rain in Zhengzhou has rung the alarm bells in major cities [5]. Located at a low latitude and close to the South China Sea, Guangzhou encounters frequent typhoons and rainstorms, and waterlogging disasters occur frequently [6,7]. In the face of short-term and sudden rainstorm disaster, disaster prevention and emergency response mechanism are particularly important, and waterlogging risk assessment is the basis of urban disaster prevention [8]. Risk assessment of urban waterlogging caused by rainstorms, so as to carry out targeted prevention and management, can effectively prevent waterlogging and minimize its negative impact.

Many scholars have conducted long-term and extensive research on urban flood disaster risk assessment. Commonly used methods include assessment based on historical disasters [9], assessment based on hydrological model [10], assessment based on indicator system [11], and assessment based on remote sensing and GIS [12]. Due to the general lack of real-time monitoring data of surface flow and waterlogging points in cities, and with the development of computer technology and geographic information systems, comprehensive risk assessment methods based on scenario simulation and analysis have received widespread attention [13]. This approach can reflect the dynamics of disasters and enable the assessment of consequences for unconventional disasters that have never occurred

before [14]. Zhang et al. [15] used a coupled hydrodynamic model to build an assessment framework for road network vulnerability to urban waterlogging, and discussed the impact of rainfall patterns on road network vulnerability. Quan et al. [16] developed a scenario-based methodology framework to predict future land-use change and its impact on flood risk. Rapid expansion of impervious surface increases surface runoff depth and could increase rainstorm flood risk in Shanghai. However, most of the above scholars focus on the cause analysis and simulation prediction of waterlogging. There is still a lack of detailed research on the combination of waterlogging simulation and disaster loss assessment.

In recent years, some scholars first put forward urban waterlogging simulation methods, such as Storm Water Management Model (SWMM) [17,18], MIKE URBAN [19], IIIU-DAS [20], the Soil Conservation Service (SCS) model [21,22] and machine learning techniques [23]. All of them have achieved good application results. The SWMM model is widely used. However, this method is one-dimensional and not suitable for simulating two-dimensional surface runoff [24]. The SCS model has the characteristics of a simple structure, few parameters and less strict requirements on observation data, so it is more suitable for small area runoff simulation without accurate data [25]. Yang et al. [26] established a multi-factor correlation model to simulate historical flood events, and the results showed that its calculation time and simulation results were better than SWMM and Mike Urban. Meng et al. [27] proposed a simple and efficient urban rainstorm inundation simulation method URIS based on GIS and the SCS model. Chen et al. [25] established the urban waterlogging disaster model by combining the rainstorm intensity formula, local surface statistics and SCS model. Mei et al. [28] designed the simulation of urban waterlogging based on the different characteristics of rainstorms, and the results show that under the condition of equal rainfall, rainfall intensity is the key factor affecting the submerged area, depth and damage.

In view of the above problems, in this paper, we propose a simulation method of the urban waterlogging process and inundation area based on the SCS model and GIS, and we conduct a simulation study on the disaster-causing factors under different rainstorm scenarios. On this basis, combined with the risk theory of natural disasters, an evaluation framework of the waterlogging disaster index system based on scenario simulation is built, and the risk evaluation model of waterlogging in Guangzhou is established. The model determines the spatial distribution of waterlogging disaster risk in Guangzhou according to the urban inundation range and inundation depth under different rainstorm scenarios, combined with the disaster-pregnant environment and disaster-bearing body.

2. Materials and Methods

2.1. Study Area

Guangzhou is located in the south-central part of Guangdong Province, China, bordering on the South China Sea, with a typical south Asian tropical monsoon climate. The annual average rainfall is more than 1500 mm, and the rainy season is concentrated from April to September. The terrain of the city is high in the northeast and low in the southwest, while the low-lying plains in the south are mostly central urban areas. The central city has a dense water network, with 231 major rivers crisscrossing it. The region has a large population density and developed economy and trade. In recent years, the annual loss caused by waterlogging has exceeded CNY 500 million.

In this paper, the digital elevation model of Guangzhou (ASTERGDEM, resolution 30 m) and land-use data were used, as shown in Figure 1. Among them, the digital elevation model (DEM) was obtained from the Geospatial Data Cloud (<http://www.gscloud.cn/>, accessed on 26 July 2022), and the land-use data were obtained from the Chinese Academy of Sciences Resource and Environmental Science and Data Center (<http://www.resdc.cn/>, accessed on 26 July 2022). Other basic geographical and topographic data, urban hydrological data and social and economic data are shown in Table 1.

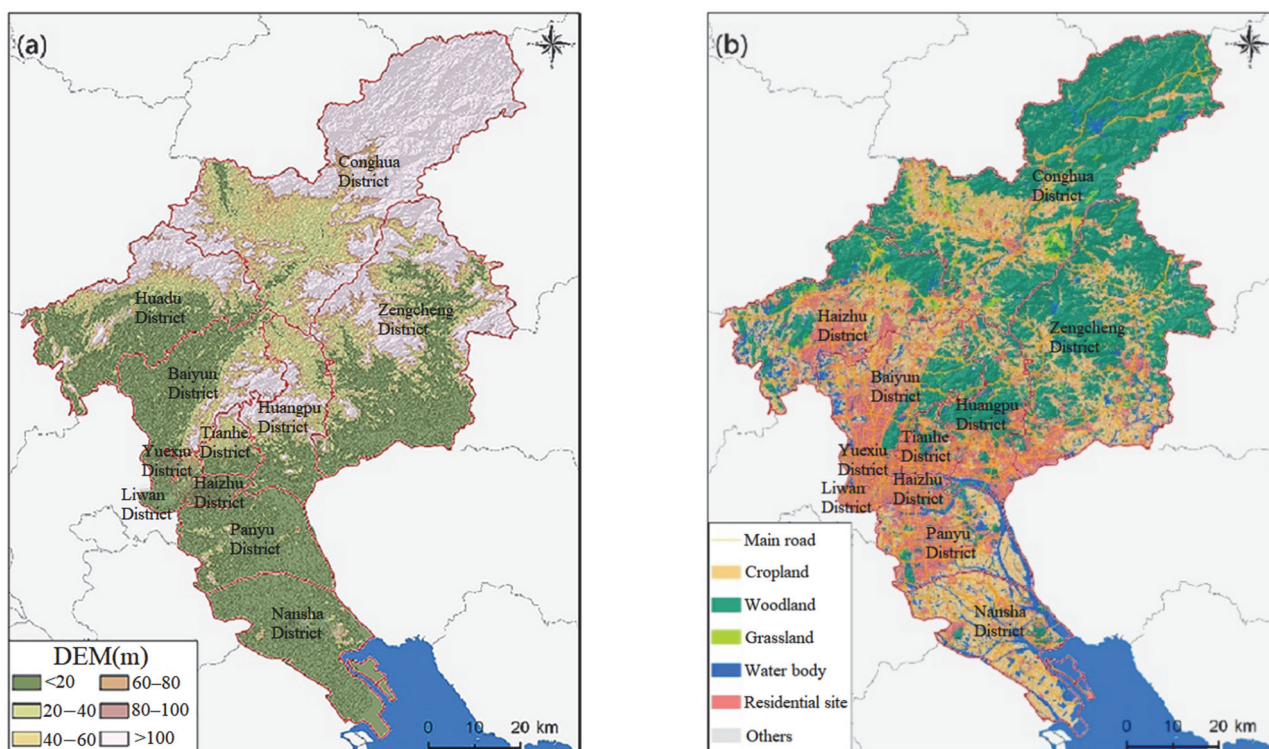


Figure 1. The digital elevation model (a) and land-use types (b) of Guangzhou.

Table 1. Basic research data.

Data	Name	Format	Remarks
Basic geographic data	River system	Shapefile	River network water system was extracted from the topographic elevation map by GIS.
	Elevation	Grid file	Extracted from DEM data.
	Residential site	Shapefile	Extracted from land-use data.
Hydrologic data	Design storm	Paper/ electronic documents	Consulted the formula for rainstorm intensity in Guangzhou and determined the parameters of the different rain types.
Socioeconomic data	Socioeconomic data of the city	Paper/ electronic documents	From the national economic and social development statistical bulletin, statistical yearbook, etc.

2.2. Risk Assessment Model of Waterlogging Disaster Based on Scenario Simulation

In this study, the urban waterlogging process and submergence area simulation method based on the SCS model and GIS were used to simulate urban waterlogging. Based on the disaster system [29] and risk triangle [30] theories, this paper selected the “risk of disaster-causing factor–sensitivity of disaster-pregnant environment–vulnerability of disaster-bearing body” evaluation framework to construct a waterlogging risk assessment model in Guangzhou. The weighted comprehensive evaluation method was used to assign a weight to each risk index, and various methods, such as the model simulation method and GIS spatial analysis method, were used to obtain the evaluation index value. Compared with the existing methods, this method adopts scenario simulation to analyze the disaster risk and evaluates the risk level of urban waterlogging by considering the vulnerability indexes of disaster-bearing bodies, such as population density and GDP density. The

overall framework of the waterlogging disaster risk assessment is shown in Figure 2. The index system of the waterlogging risk evaluation is as follows:

$$R_T = \omega_1 \times R_1 + \omega_2 \times R_2 + \omega_3 \times R_3 \tag{1}$$

where R_T is the risk index; R_1 is the risk of a disaster-causing factor; R_2 is sensitivity of the disaster-pregnant environment; R_3 is the vulnerability of the disaster-bearing body; and ω_1 , ω_2 and ω_3 are the corresponding weights of each index, respectively.

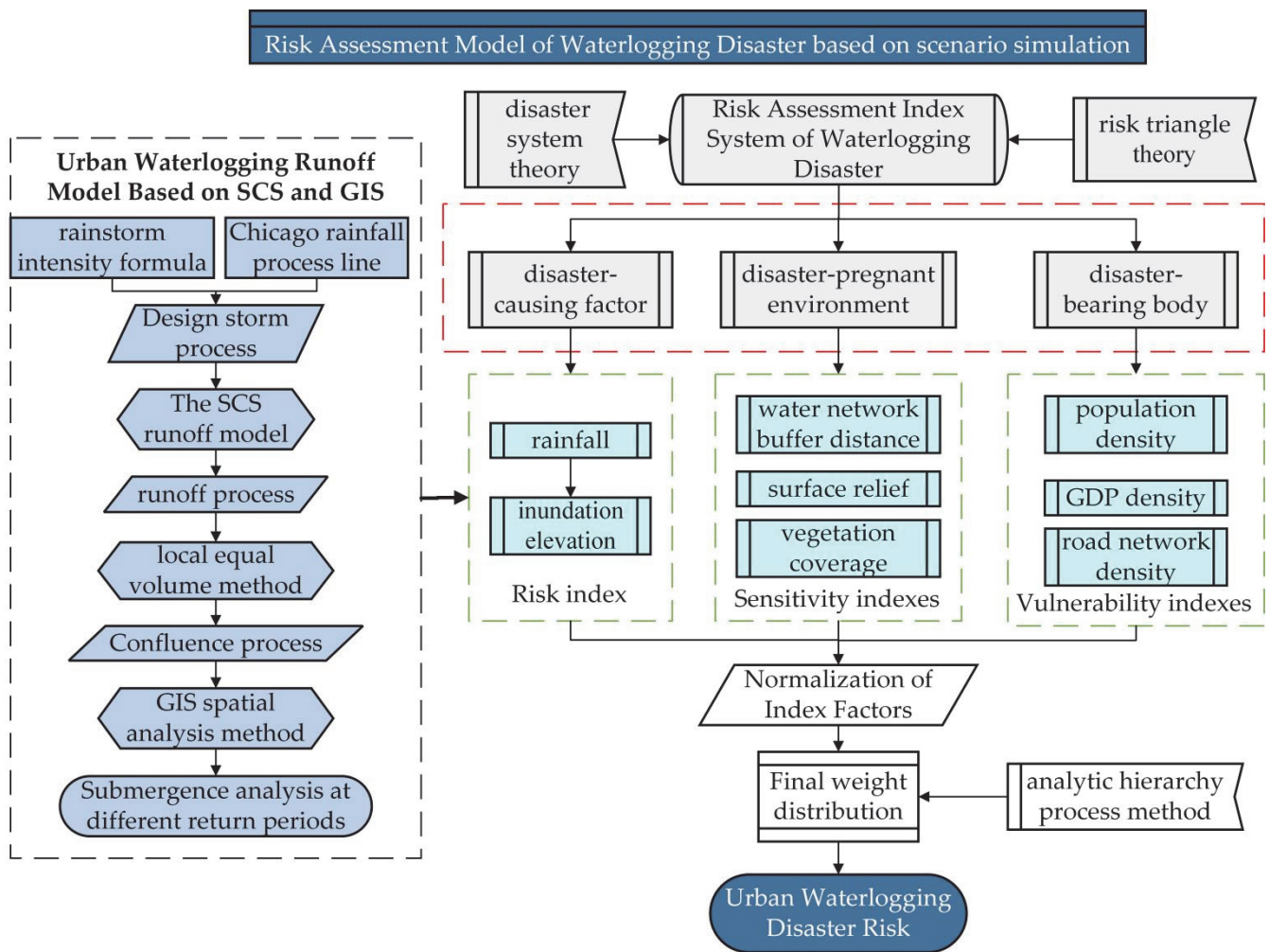


Figure 2. The overall framework of waterlogging disaster risk assessment.

2.3. Urban Waterlogging Runoff Model Based on SCS

The simulation of the urban waterlogging process includes two parts, namely, the runoff generation process and confluence process. By collecting the basic data of the basin, the rainfall and runoff models that conform to the characteristics of Guangzhou were selected to simulate the inundation process under different rainfall scenarios in different return periods. In this study, the rainstorm intensity formula and Chicago rainfall hydrograph model were used to construct the rainfall model and simulate the rainfall process. The SCS runoff generation model was used to simulate the runoff generation process, and the inundation process of urban waterlogging confluence was simulated by considering the pumping capacity and local isometric method. The inundation analysis of the rainstorms in different rainfall return periods was carried out with GIS technology.

2.3.1. Design Rainstorm Process Line

In this paper, the internationally used Chicago rain pattern is adopted, and the designed rainstorm intensity was calculated according to the rainstorm intensity Formula (2) in the “Rainstorm Formula and Calculation Chart of Guangzhou Central City” was newly revised by Guangzhou Water Authority in December 2011. The Chicago instantaneous rainstorm intensity Formula (3) was introduced into the rainstorm duration distribution [31].

$$q = \frac{3618.427(1 + 0.438 \log_{10} P)}{(t + 11.259)^{0.75}} \tag{2}$$

$$\begin{cases} i_a = \frac{(1-n)r^n A(1+C \log_{10} P)}{(t_a-t+rb)^n} + \frac{nbr^{n+1} A(1+C \log_{10} P)}{(t_a-t+rb)^{n+1}} & 0 \leq t \leq t_a \\ i_b = \frac{(1-n)(1-r)^n A(1+C \log_{10} P)}{[t-t_a+(1-r)b]^n} + \frac{nb(1-r)^{n+1} A(1+C \log_{10} P)}{[t-t_a+(1-r)b]^{n+1}} \end{cases} \tag{3}$$

where, q is the design rainstorm intensity, L/(s·ha); t is rainfall duration, min; P is the design return period, a; A, n, b, C are the parameters in the latest rainstorm formula, $A = 3618.427, n = 0.75, b = 11.259, C = 0.438$; i_a is the pre-peak instantaneous rainfall intensity, mm/min; i_b is the post-peak instantaneous rainfall intensity, mm/min; t_a is the pre-peak duration, min; t_b is post-peak duration, min; r is the relative position of rain peak.

In this paper, the duration of rainfall is selected as 120 min, the simulation time is from the beginning of the rainfall to 2 h after the end of rainfall, a total of 4 h, the rain peak coefficient $r = 0.4$, and the rainfall return period p is taken as 5 years, 10 years, 20 years, and 50 years, respectively. The design rainfall hydrographs of different return periods are shown in Figure 3.

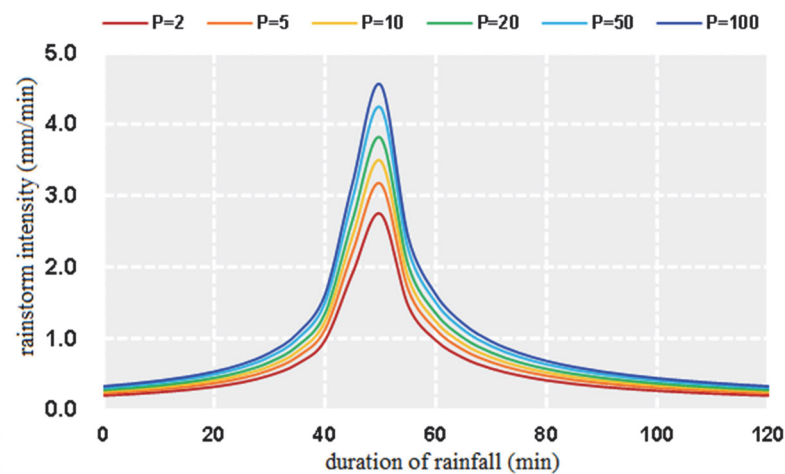


Figure 3. Design rainfall hydrograph.

2.3.2. Urban Waterlogging and Runoff Simulation Based on SCS

The SCS runoff model was proposed in the 1950s and applied to runoff simulation in small watersheds by the USDA Soil Conservation Service [32]. Based on the rainfall–runoff relationship, considering the underlying surface conditions and the water balance equation, the SCS runoff model divides the runoff process into four processes: infiltration, filling of depressions, evaporation and runoff [33].

After the surface runoff is generated in the urban area, the process of collecting the runoff from various places to the outlet section of the watershed is called the confluence. In this paper, the urban drainage capacity is considered, and the entire submerged area is considered to be in a passive submerged state, and the difference between the runoff and the pumping capacity of the pumping station is the total amount of confluence. According to the total amount of confluence in the watershed, this project uses the “GIS-based local equal volume method” to simulate the flooding situation of the city. The method divides the

study into several small catchment areas, and the rainfall and runoff are simulated in these small catchment areas, and finally the confluence is carried out at the exit of the catchment area, which finally reflects the flooding status of the urban area [34]. The calculation flow of the local equal volume method is shown in Figure 4.

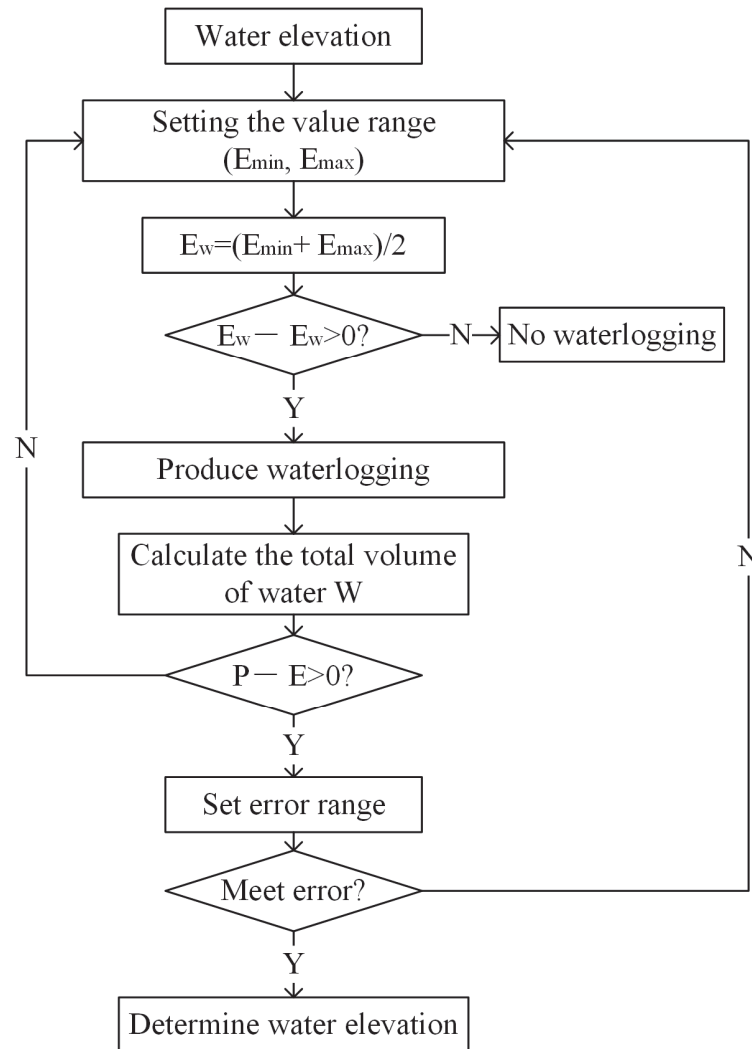


Figure 4. Flow chart of the local equal volume algorithm.

2.4. Risk Assessment Index System

2.4.1. Construction of Evaluation Index System

Urban waterlogging is mainly caused by excessive rainfall in a short period of time, which exceeds the drainage capacity of the city, leading to water on the road and causing local submergence. Therefore, precipitation is the main disaster factor causing waterlogging. Sun et al. [35] evaluated urban waterlogging risk by integrating hazard intensity index, socioeconomic exposure index, and urban adaptability index. Roy et al. [36] summarized the waterlogging risk into waterlogging conditioning factors and waterlogging vulnerability indicators. In this paper, rainfall (P_1) is selected as the evaluation index of the disaster-causing factor (R_1), and the submerging water depth under a 5-year rainfall scenario is simulated as the basis for dividing the risk spatial distribution of the disaster-causing factor through the submerging simulation of the SCS runoff generation model and GIS local equal volume passive submerging algorithm.

As the transmission carrier of the disaster system, the disaster-pregnant environment promotes the disaster-causing factor to transfer the destructive effect to the disaster-bearing

body [36]. The disaster-pregnant environment of the waterlogging disasters can be divided into the natural environment and social environment. Natural environmental factors include meteorology, topography, hydrology and water system characteristics, vegetation coverage factors, etc. [37,38]. Social environmental factors include flood-prone area ratio, population number and population density, number of reservoirs and ponds, building density, per capita income, etc. [35,39]. After comprehensive evaluation of the sensitivity of various environmental factors, the water network buffer distance (P_2) [40], surface relief (P_3) and vegetation coverage (P_4), which have strong influence on the sensitivity of runoff, were selected as the evaluation indexes of the sensitivity of disaster-pregnant environment (R_2). The water network buffer distance represents the distance from the water network. The closer it is, the greater the risk of inundation.

The vulnerability of the disaster-bearing body refers to the possible loss of the disaster-bearing body under a certain intensity of a disaster-causing factor, mainly including casualties and economic losses. The vulnerability of personnel is measured by population density (P_5); economic vulnerability is mainly measured by GDP density (P_6) and road network density (P_7). Based on the above indicators, the urban waterlogging disaster risk assessment index system was established, as shown in Table 2.

Table 2. Risk assessment index system for urban waterlogging disasters.

First-Level Indexes	Second-Level Indexes	Specific Indexes
Urban waterlogging disaster risk (R_T)	Risk of disaster-causing factor (R_1)	Rainfall (P_1)
	Sensitivity of disaster-pregnant environment (R_2)	Water network buffer distance (P_2)
		Surface relief (P_3)
	Vulnerability of disaster-bearing body (R_3)	Vegetation coverage (P_4)
Population density (P_5)		
GDP density (P_6)		
		Road network density (P_7)

2.4.2. Normalization of Index Factors

This paper adopts the weighted comprehensive evaluation method to comprehensively evaluate each risk indicator. This method is a comprehensive analysis and evaluation method for multiple impact factors, which not only considers the impact factor of each indicator, but also comprehensively evaluates the impact degree of each indicator on the evaluation object. The specific formula is as follows:

$$R = \sum_{i=1}^n \omega_i \times P_i \tag{4}$$

where R is the comprehensive risk value; i is each evaluation index; and P_i and w_i are the impact factor of i and its corresponding weight, respectively.

When dealing with different disaster indexes, different data have different dimensions. Direct superposition cannot reflect the real impact of data, so each index needs to be processed in a dimensionless manner. For the positive index, the bigger the index value, the greater the disaster risk, which belongs to the maximum optimal type; the calculation formula is as follows:

$$X'_{ij} = \frac{X_{ij} - X_{i,\min}}{X_{i,\max} - X_{i,\min}} \tag{5}$$

For the negative index, the bigger the index value, the smaller the disaster risk, which belongs to the minimum optimal type; the calculation formula is as follows:

$$X'_{ij} = \frac{X_{i,\max} - X_{ij}}{X_{i,\max} - X_{i,\min}} \tag{6}$$

where X_{ij} is the j index of the i object; X'_{ij} is the value of the j index of the i object after dimensionless processing; and $X_{i,\max}$ and $X_{i,\min}$ are the maximum and minimum value of

this index, respectively. According to the above formula, the range of the dimensionless treatment is (0,1).

2.4.3. Weight Analysis of Evaluation Indexes

Weight is a physical quantity that measures the contribution degree of each index and criterion layer to its target layer. In the process of multi-index modeling, weight assignment is an inevitable problem. In the numerous index evaluation system, the weight design methods include the Delphi method, empirical weight method, mathematical statistics method, fuzzy statistics method, and analytic hierarchy process (AHP). AHP is a method that combines qualitative and quantitative methods. It treats people's subjective judgments with mathematical expressions and examines and reduces the subjective influence on a certain extent. It can effectively solve multi-objective complex problems [41].

As the analytic hierarchy process is a subjective weighting method, the evaluation results may be biased due to human subjective factors, and the problem of inconsistency of target is prone to occur in the process of constructing judgment matrix through pair comparison [42]. Based on the judgment matrix, composed of the evaluation index values, the weight of indexes can be determined by using the order degree of the system information reflected by the information entropy and its utility [43]. The larger the difference between the values of the evaluation objects on a certain index, the smaller the entropy value, the greater the amount of effective information provided by the index, the greater the effect on decision making, and the bigger the weight should be. Referring to [36,41,43], the judgment matrices of the analytic hierarchy process in this study are, respectively, set as

$$R_T = \begin{bmatrix} 1 & 2 & 1.5 \\ 0.5 & 1 & 0.8 \\ 0.67 & 1.25 & 1 \end{bmatrix} \quad R_2 = \begin{bmatrix} 1 & 3 & 5 \\ 0.33 & 1 & 2 \\ 0.2 & 0.5 & 1 \end{bmatrix} \quad R_3 = \begin{bmatrix} 1 & 0.67 & 0.67 \\ 1.5 & 1 & 1.2 \\ 1.5 & 0.3 & 1 \end{bmatrix} \quad (7)$$

The calculated consistency ratios (CR) were 0.0004, 0.0032 and 0.0032, respectively, which were all less than 0.1, indicating that the consistency of the judgment matrix was acceptable. The final weight of each index is determined as shown in Table 3.

Table 3. Urban waterlogging risk assessment indicators and weights.

Factors	Indexes	Weights
Risk of disaster-causing factor (0.482)	Rainfall (P_1)	1.00
	Water network buffer distance (P_2)	0.66
Sensitivity of disaster-pregnant environment (0.226)	Surface relief (P_3)	0.21
	Vegetation coverage (P_4)	0.12
	Population density (P_5)	0.27
Vulnerability of disaster-bearing body (0.291)	GDP density (P_6)	0.38
	Road network density (P_7)	0.34

3. Result and Analysis

3.1. Submerged Scenario Simulation

Based on the maximum possible water retention in the basin and the calculation formula of the SCS runoff model, the spatial distribution of runoff depth in Guangzhou under different rainfall scenarios is depicted in Figure 5, and the runoff results are shown in Table 4. It can be seen from the calculation results that the maximum rainfall reaches 126.0 mm, the corresponding runoff depth is 60.5 mm, the minimum rainfall is 76.0 mm and the corresponding runoff depth is 26.5 mm.

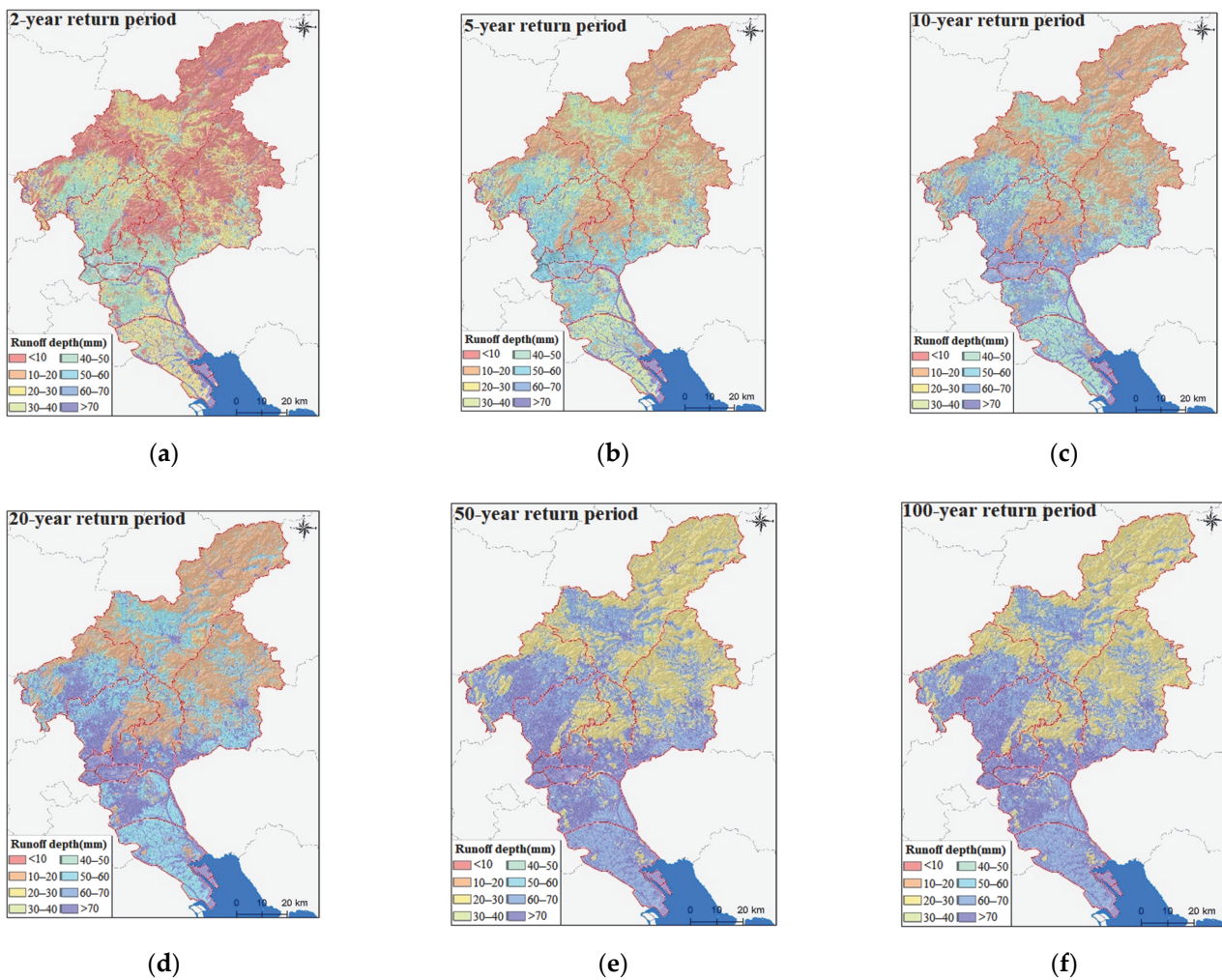


Figure 5. Spatial distribution of runoff depth under different precipitation scenarios.

Table 4. Runoff statistics of falling water under different scenarios.

Rainfall Return Period (a)	2	5	10	20	50	100
Rainfall (mm)	76.0	87.8	96.6	105.5	117.2	126.0
Rain peak (mm/min)	2.75	3.17	3.49	3.81	4.24	4.56
Runoff depth (mm)	26.5	33.8	39.6	45.7	54.0	60.5

According to the rainfall distribution of different rainfall return periods, the local equal volume method and ArcGIS spatial analysis tools were used to carry out inundation analysis and calculations, and the distribution map of the inundation area of Guangzhou under different rainfall return periods was obtained (Figure 6). The water volume and submerged elevation of urban waterlogging are shown in Table 5. The water area of Guangzhou is about 544.9 km², accounting for about 7.3% of the area of Guangzhou, and it is mostly concentrated in the southern area, mainly rivers, canals, reservoirs, ponds and beaches, which can alleviate the impact of rainstorms to a certain extent. According to the distribution map of waterlogging inundation in different rainfall return periods, for the rainstorms with different rainfall return periods, the initial submerged area is the same, then spreading to the surrounding areas in a plane shape. The longer the rainfall return period, the wider the area submerged in water, the deeper the water elevation and the greater the impact. Under the influence of a 2-year return rainfall period, the submerged area is about 79.1 km² (excluding the original water body area), and under the

influence of a 100-year return torrential rain period, the increased area is 126.3 km². From the approximate linear relationship, when the 2 h precipitation is less than 100 mm, the submerged area increases by 3.4 km² for every 10 mm increase in precipitation; when the 2 h precipitation is greater than 100 mm, the inundation area increases by 18 km² for every 10 mm increase in precipitation.

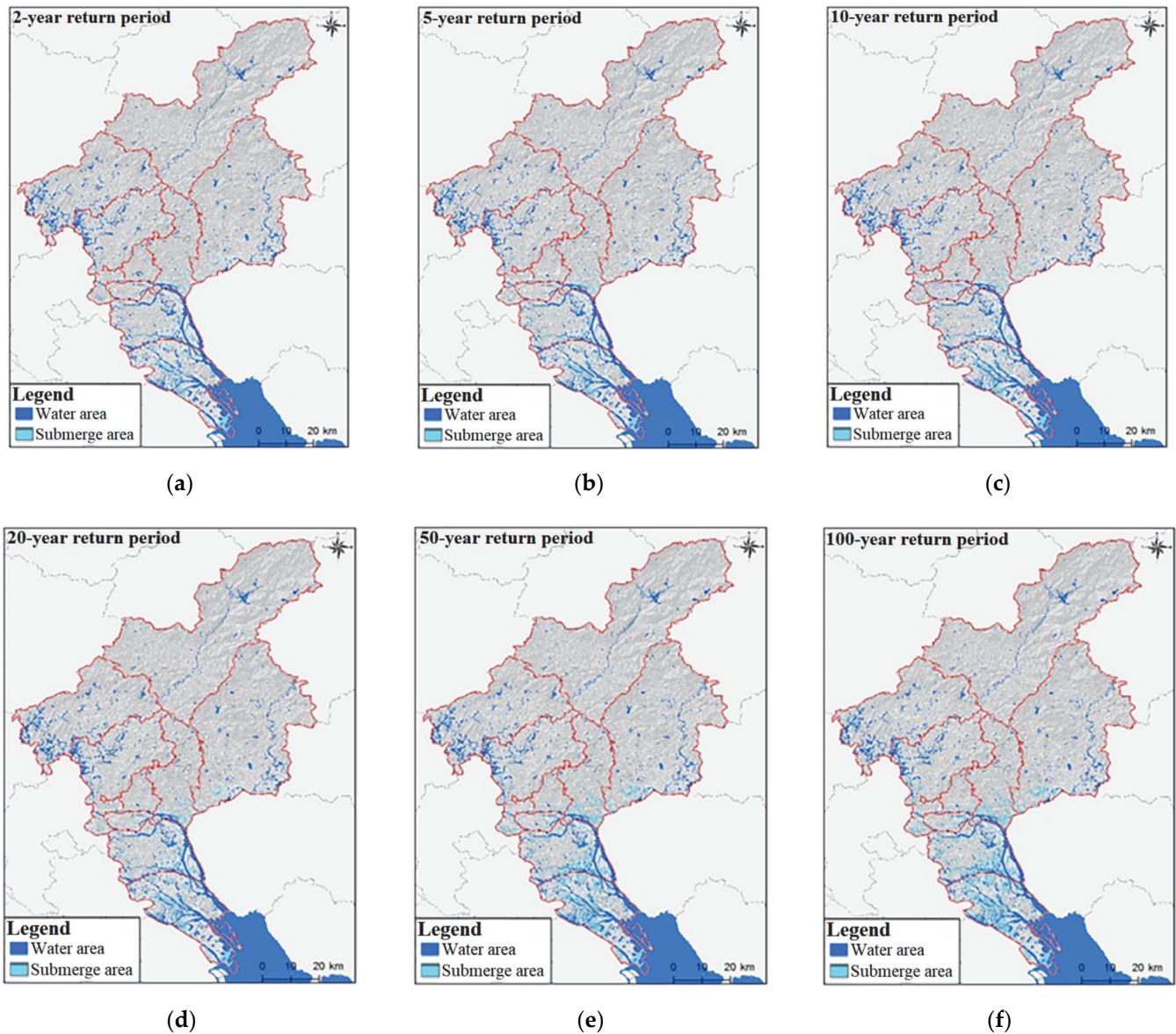


Figure 6. Inundation range under different precipitation scenarios.

Table 5. Waterlogging volume and inundation elevation in different rainfall return periods.

Rainfall Return Period (a)	2	5	10	20	50	100
Rainfall (mm)	26.5	33.8	39.6	45.7	54.0	60.5
Waterlogging volume (10 ⁴ m ³)	19,018.4	24,261.0	28,404.5	32,769.0	38,738.4	43,379.1
Elevation (m)	1.55	1.74	1.88	2.03	2.23	2.39

3.2. Risk Analysis of the Disaster-Causing Factors

In this study, the net rainfall under the rainfall scenario for which the return period is 5 years was used to measure the risk of disaster-causing factors in urban waterlogging,

and the SCS runoff model and normalization method were used to obtain the spatial distribution map of the risk of disaster-causing factors, as shown in Figure 7. It can be seen from the figure that the areas with a higher risk are mainly located in Liwan District, Yuexiu District and Haizhu District, and the spatial mean of the risk index is 0.650, 0.623 and 0.587, respectively.



Figure 7. Spatial distribution of hazard factors in Guangzhou.

3.3. Sensitivity Assessment of the Disaster-Pregnant Environment

According to the indicators in Table 2, the sensitivity of the disaster-pregnant environment includes three aspects: the water network buffer distance, surface relief and vegetation coverage. Water network buffer distance is measured by Euclidean distance, which can be calculated by using the tool Euclidean Distance in Arcgis10.2. The closer the distance to the water body, the greater the risk of being submerged. Surface relief is the elevation difference in a region, which can be calculated with the Neighborhood Statistic tool in ArcGIS 10.2. The smaller surface relief is—a relatively flat terrain—the less likely it is to form ponding. Vegetation coverage was calculated using remote sensing image data provided by Landsat-8. Since plantations can effectively discharge and store floods, in general, the higher the vegetation coverage, the lower the sensitivity of the disaster-pregnant environment. The normalized spatial distribution of the above indicators is shown in Figure 8a–c. Using the weighted summation of $R_2 = 0.66P_2 + 0.21P_3 + 0.12P_4$, the sensitivity assessment results of the disaster-pregnant environment were obtained (Figure 8d). From the evaluation results, the sensitivity of the disaster-pregnant environment in the south of Guangzhou is relatively high, mainly because of the relatively high water network density, gentle terrain and low vegetation coverage in this area.

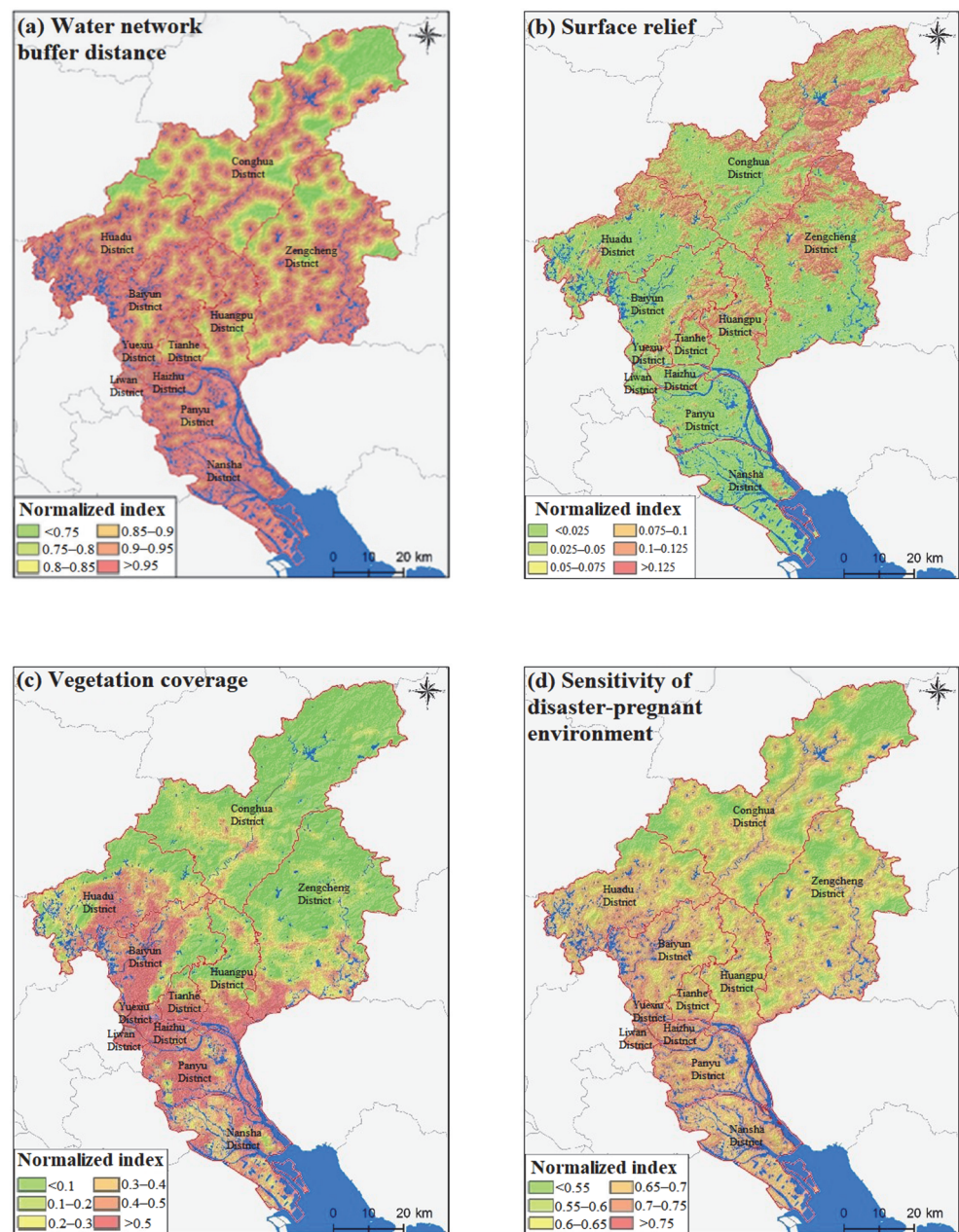


Figure 8. Sub indicators and comprehensive evaluation of environmental sensitivity to disasters.

3.4. Vulnerability Assessment of the Disaster-Bearing Body

According to indicators in Table 2, the vulnerability of the disaster-bearing body includes population density, GDP density and road network density. Population density and GDP density were obtained from “China’s Population Spatial Distribution Kilometer Grid” data set, “China’s GDP Spatial Distribution Kilometer Grid” data set and the Guangzhou Statistical Yearbook. The important manifestation of urban waterlogging disasters is affecting the safety of residents in the region. A population index is very important in the vulnerability assessment of disaster-bearing bodies. The more densely populated the disaster-bearing bodies are, the higher the vulnerability is. Similarly, GDP reflects the economic development of a basin. The higher the GDP value is, the greater the economic loss base and the higher the disaster risk will be in case of a waterlogging disaster. Road traffic is an important part of urban infrastructure construction. From the above analysis, the road traffic network is an important carrier of various urban systems. When disasters occur, areas with a low density have a low risk of disaster, while areas with a high density

have a higher risk of disaster. The normalized spatial distribution of the above indicators is shown in Figure 9a–c. After weighted sum of $R_3 = 0.27P_5 + 0.38P_6 + 0.34P_7$, the vulnerability assessment result of the disaster-bearing body was obtained (Figure 9d). According to the evaluation results, Liwan District, Haizhu District, Yuexiu District and Tianhe District have higher vulnerability to a disaster-bearing body, mainly because of population aggregation due to the relatively developed economy in these districts.

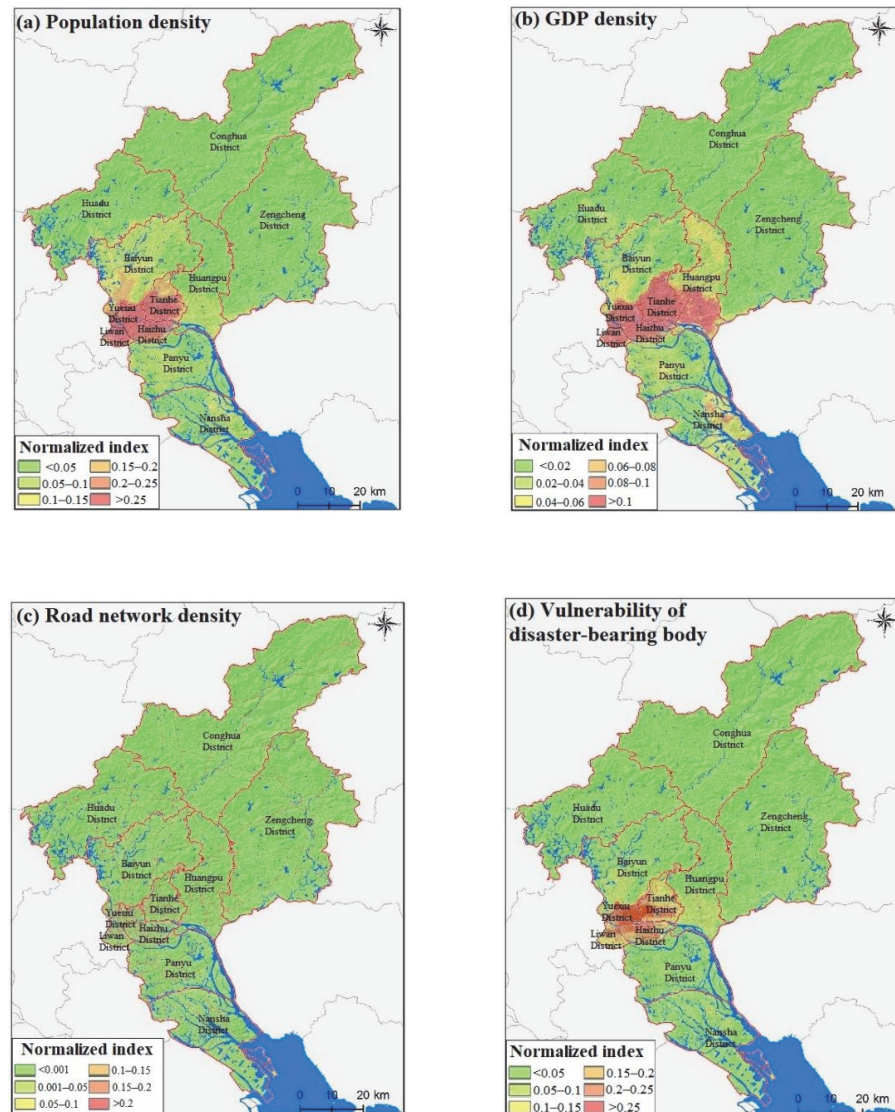


Figure 9. Sub-indicators and comprehensive evaluation of the vulnerability of the disaster-bearing body.

3.5. Urban Waterlogging Disaster Risk Assessment

According to the results of the above mentioned, the risk of a disaster-causing factor (R_1), the sensitivity of the disaster-pregnant environment (R_2) and the vulnerability of disaster-bearing body (R_3), combined with the set weights, and according to $R_T = 0.482R_1 + 0.226R_2 + 0.291R_3$, a comprehensive index of the waterlogging disaster risk in Guangzhou was calculated (Figure 10a). The optimal segmentation method was used to segment all samples, and the optimal classification level and threshold of the urban waterlogging disaster risk in the study area were determined. Corresponding to the risk level of urban waterlogging disasters, the risk levels of the urban waterlogging disasters in the study area were determined as a low waterlogging disaster risk, medium-low waterlogging risk,

medium waterlogging risk, medium-high waterlogging risk and high waterlogging risk, and the corresponding comprehensive risk index ranges were (0, 0.224), (0.224, 0.382), (0.382, 0.546), (0.546, 0.673) and (0.673, 1); the divided risk levels are shown in Figure 10b. According to statistics, Guangzhou has a low flood risk, medium-low flood risk, medium flood risk, medium-high waterlogging risk and high waterlogging risk areas of 3084.4 km², 2032.8 km², 1070.7 km², 273.2 km² and 168.1 km², respectively (excluding water body area), of which the total area of medium-high waterlogging risk and high waterlogging risk accounts for 6.7%, mainly concentrated in Yuexiu District, Liwan District, Haizhu District and Tianhe District. The results are strongly consistent with the historical flood disaster situation in Guangzhou [6] and with the assessment of waterlogging disaster risk in Guangzhou in [7]. However, this study also considers the impact of population density and GDP density on the risk of waterlogging disaster, so the assessment results in areas with a high population density are higher than those in [7], especially in Yuexiu District and Liwan District, where the areas of medium-high risk and above accounted for more than 90% of the corresponding districts (Figure 11).

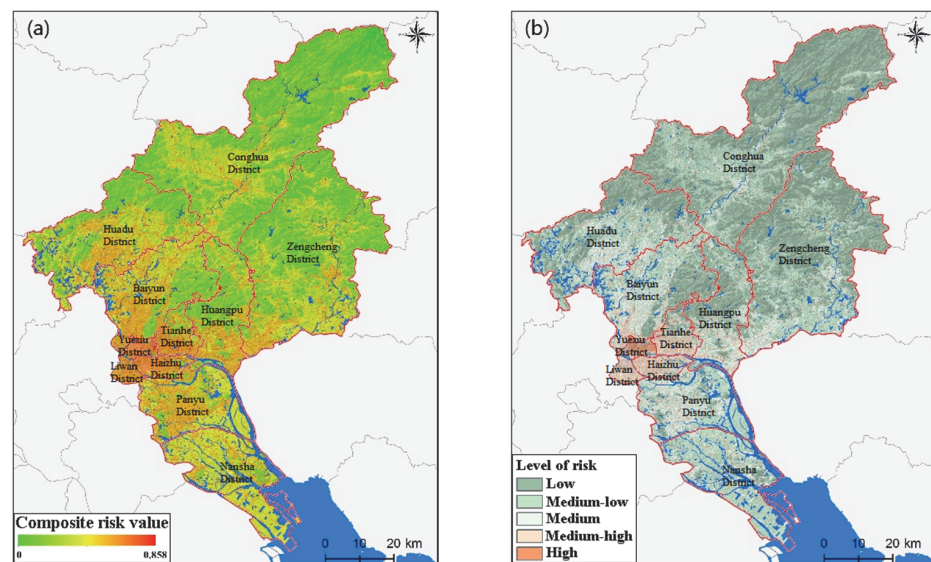


Figure 10. Spatial distribution (a) and grade division (b) of the comprehensive index of waterlogging disaster risk in Guangzhou.

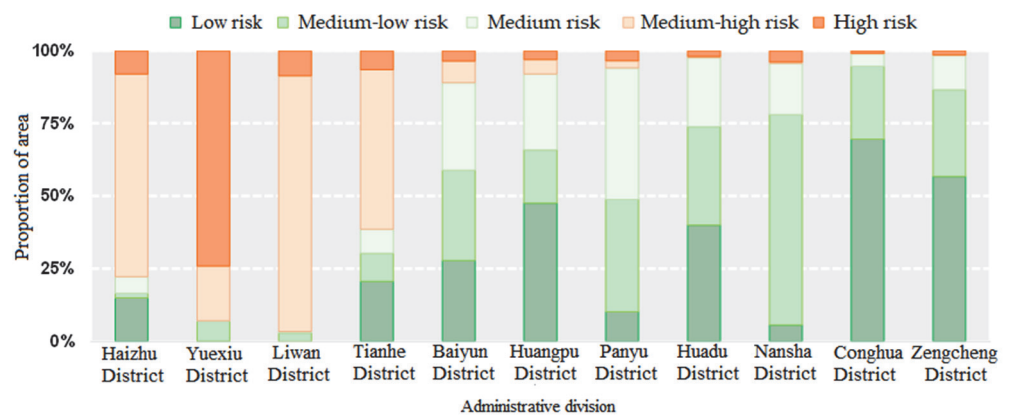


Figure 11. Statistics of the waterlogging disaster risk levels in various administrative regions of Guangzhou.

4. Conclusions

In this paper, through the simulation of inundation scenarios under different rainfall return periods in Guangzhou, it can be seen that the inundation of torrential rain spreads

to the surrounding areas in a planar manner. For the 2-year rainfall return period, the inundation range is about 79.1 km² (excluding the original water body area), and the inundation elevation is about 1.55 m; in case of a once-in-a-century torrential rain, the submerged depth can reach 2.39 m, and the submerged range will increase to 126.3 km². There is a nearly linear relationship between rainfall and the inundation range. When the 2 h precipitation is less than 100 mm, the inundation range increases by 3.4 km² for every 10 mm increase in precipitation; when the 2 h precipitation is greater than 100 mm, the inundation range increases by 18 km² for every 10 mm increase in precipitation. At the same time, this paper builds a comprehensive risk assessment model for urban waterlogging disasters in Guangzhou. The results show that the areas of low waterlogging risk, medium-low waterlogging risk, medium waterlogging risk, medium-high waterlogging risk and high waterlogging risk in Guangzhou are 3084.4 km², 2032.8 km², 1070.7 km², 273.2 km² and 168.1 km² (without water body area), respectively, among which the total area of medium-high waterlogging risk and high waterlogging risk accounts for 6.7%, mainly concentrated in Yuexiu District, Liwan District, Haizhu District and Tianhe District.

This method considers the disaster risk caused by urban waterlogging from many aspects and can evaluate the consequences of unconventional disasters that have never occurred before. The results of the risk assessment can provide a basis for the scientific decision making of disaster prevention and mitigation in Guangzhou, and have important practical significance for the rational allocation of disaster prevention and mitigation resources and waterlogging control. Although this study analyzed the impact of flood disaster from various factors, some factors were still taken into consideration, such as an impervious road surface and rainfall duration. In addition, some novel methods can be incorporated into future research to assess the risk of waterlogging. For example, machine learning can be used to evaluate the probability of waterlogging, and convolutional neural networks can be used to consider the neighborhood effects of waterlogging.

Author Contributions: Conceptualization, Z.Y.; data curation, S.X. and H.Z.; formal analysis, S.X. and W.L.; investigation, H.Z. and H.L.; methodology, S.X. and Z.Y.; project administration, Y.W.; resources, Y.W.; software, Z.Y.; validation, W.L. and H.L.; visualization, W.L.; writing—original draft, W.L.; writing—review & editing, S.X. and W.L.; supervision, Y.W. All authors have read and agreed to the published version of the manuscript.

Funding: This research was funded by the Water Conservancy Science and Technology Innovation project of the Guangdong Province, grant number 2017-03, and the Major Key Technology Research Project of Water Conservancy grant number SKR-2022007.

Data Availability Statement: Not applicable.

Conflicts of Interest: The authors declare no conflict of interest.

References

1. O’Gorman, P.A. Precipitation Extremes Under Climate Change. *Curr. Clim. Chang. Rep.* **2015**, *1*, 49–59. [[CrossRef](#)] [[PubMed](#)]
2. Qiu, J. Urbanization contributed to Beijing storms. *Nature* **2012**, *10*, 11086. [[CrossRef](#)]
3. Jiang, Y.; Zevenbergen, C.; Ma, Y. Urban pluvial flooding and stormwater management: A contemporary review of China’s challenges and “sponge cities” strategy. *Environ. Sci. Policy* **2018**, *80*, 132–143. [[CrossRef](#)]
4. Du, S.; Gu, H.; Wen, J.; Chen, K.; Van Rompaey, A. Detecting Flood Variations in Shanghai over 1949–2009 with Mann-Kendall Tests and a Newspaper-Based Database. *Water* **2015**, *7*, 1808–1824. [[CrossRef](#)]
5. Wang, J.; Hu, C.; Ma, B.; Mu, X. Rapid Urbanization Impact on the Hydrological Processes in Zhengzhou, China. *Water* **2020**, *12*, 1870. [[CrossRef](#)]
6. Zhang, Q.; Wu, Z.; Zhang, H.; Dalla Fontana, G.; Tarolli, P. Identifying dominant factors of waterlogging events in metropolitan coastal cities: The case study of Guangzhou, China. *J. Environ. Manag.* **2020**, *271*, 110951. [[CrossRef](#)]
7. Shu, Y.; Zheng, G.; Yan, X. Application of Multiple Geographical Units Convolutional Neural Network based on neighborhood effects in urban waterlogging risk assessment in the city of Guangzhou, China. *Phys. Chem. Earth Parts A B C* **2022**, *126*, 103504. [[CrossRef](#)]
8. Lin, T.; Liu, X.; Song, J.; Zhang, G.; Jia, Y.; Tu, Z.; Zheng, Z.; Liu, C. Urban waterlogging risk assessment based on internet open data: A case study in China. *Habitat Int.* **2018**, *71*, 88–96. [[CrossRef](#)]

9. Wang, Y.; Zhai, J.; Song, L. Waterlogging risk assessment of the Beijing-Tianjin-Hebei urban agglomeration in the past 60 years. *Theor. Appl. Climatol.* **2021**, *145*, 1039–1051. [[CrossRef](#)]
10. Xue, F.; Huang, M.; Wang, W.; Zou, L. Numerical Simulation of Urban Waterlogging Based on FloodArea Model. *Adv. Meteorol.* **2016**, *2016*, 3940707. [[CrossRef](#)]
11. Liu, Z.; Jiang, Z.; Xu, C.; Cai, G.; Zhan, J. Assessment of provincial waterlogging risk based on entropy weight TOPSIS-PCA method. *Nat. Hazards* **2021**, *108*, 1545–1567. [[CrossRef](#)]
12. Zhou, M.; Feng, X.; Liu, K.; Zhang, C.; Xie, L.; Wu, X. An Alternative Risk Assessment Model of Urban Waterlogging: A Case Study of Ningbo City. *Sustainability* **2021**, *13*, 826. [[CrossRef](#)]
13. Quan, R.-S. Rainstorm waterlogging risk assessment in central urban area of Shanghai based on multiple scenario simulation. *Nat. Hazards* **2014**, *73*, 1569–1585. [[CrossRef](#)]
14. Boni, S.; Hong, H.; Nan, Z. Dynamic urban waterlogging risk assessment method based on scenario simulations. *J. Tsinghua Univ. Sci. Technol.* **2015**, *55*, 684–690.
15. Zhang, M.; Xu, M.; Wang, Z.; Lai, C. Assessment of the vulnerability of road networks to urban waterlogging based on a coupled hydrodynamic model. *J. Hydrol.* **2021**, *603*, 127105. [[CrossRef](#)]
16. Quan, R. Impact of future land use change on pluvial flood risk based on scenario simulation: A case study in Shanghai, China. *Arab. J. Geosci.* **2021**, *14*, 943. [[CrossRef](#)]
17. Bisht, D.S.; Chatterjee, C.; Kalakoti, S.; Upadhyay, P.; Sahoo, M.; Panda, A. Modeling urban floods and drainage using SWMM and MIKE URBAN: A case study. *Nat. Hazards* **2016**, *84*, 749–776. [[CrossRef](#)]
18. Rabori, A.M.; Ghazavi, R. Urban Flood Estimation and Evaluation of the Performance of an Urban Drainage System in a Semi-Arid Urban Area Using SWMM. *Water Environ. Res.* **2018**, *90*, 2075–2082. [[CrossRef](#)]
19. Sarkar, S.K.; Rahman, M.A.; Esraz-Ul-Zannat, M.; Islam, M.F. Simulation-based modeling of urban waterlogging in Khulna City. *J. Water Clim. Chang.* **2021**, *12*, 566–579. [[CrossRef](#)]
20. Tsihrintzis, V.A.; Sidan, C.B. ILLUDAS and PSRM-QUAL predictive ability in small urban areas and comparison with other models. *Hydrol. Processes* **2008**, *22*, 3321–3336. [[CrossRef](#)]
21. Yu, H.; Zhao, Y.; Fu, Y. Optimization of Impervious Surface Space Layout for Prevention of Urban Rainstorm Waterlogging: A Case Study of Guangzhou, China. *Int. J. Environ. Res. Public Health* **2019**, *16*, 3613. [[CrossRef](#)] [[PubMed](#)]
22. Suribabu, C.R.; Bhaskar, J. Evaluation of urban growth effects on surface runoff using SCS-CN method and Green-Ampt infiltration model. *Earth Sci. Inform.* **2015**, *8*, 609–626. [[CrossRef](#)]
23. Darabi, H.; Choubin, B.; Rahmati, O.; Torabi Haghighi, A.; Pradhan, B.; Kløve, B. Urban flood risk mapping using the GARP and QUEST models: A comparative study of machine learning techniques. *J. Hydrol.* **2019**, *569*, 142–154. [[CrossRef](#)]
24. Zhao, L.; Zhang, T.; Fu, J.; Li, J.; Cao, Z.; Feng, P. Risk Assessment of Urban Floods Based on a SWMM-MIKE21-Coupled Model Using GF-2 Data. *Remote Sens.* **2021**, *13*, 4381. [[CrossRef](#)]
25. Chen, Z.; Li, K.; Du, J.; Chen, Y.; Liu, R.; Wang, Y. Three-dimensional simulation of regional urban waterlogging based on high-precision DEM model. *Nat. Hazards* **2021**, *108*, 2653–2677. [[CrossRef](#)]
26. Yang, Y.; Pan, C.; Fan, G.; Tian, M.; Wang, J. A New Urban Waterlogging Simulation Method Based on Multi-Factor Correlation. *Water* **2022**, *14*, 1421. [[CrossRef](#)]
27. Meng, X.; Zhang, M.; Wen, J.; Du, S.; Xu, H.; Wang, L.; Yang, Y. A Simple GIS-Based Model for Urban Rainstorm Inundation Simulation. *Sustainability* **2019**, *11*, 2830. [[CrossRef](#)]
28. Mei, C.; Liu, J.; Wang, H.; Li, Z.; Yang, Z.; Shao, W.; Ding, X.; Weng, B.; Yu, Y.; Yan, D. Urban flood inundation and damage assessment based on numerical simulations of design rainstorms with different characteristics. *Sci. China Technol. Sci.* **2020**, *63*, 2292–2304. [[CrossRef](#)]
29. Yang, P.; Huang, X.; Peng, L.; Zheng, Z.; Wu, X.; Xing, C. Safety evaluation of major hazard installations based on regional disaster system theory. *J. Loss Prev. Process Ind.* **2021**, *69*, 104346. [[CrossRef](#)]
30. Crichton, D. The risk triangle. *Nat. Disaster Manag.* **1999**, *102*, 17.
31. Liao, D.; Zhang, Q.; Wang, Y.; Zhu, H.; Sun, J. Study of Four Rainstorm Design Methods in Chongqing. *Front. Environ. Sci.* **2021**, *9*, 51. [[CrossRef](#)]
32. Xiao, B.; Wang, Q.-H.; Fan, J.; Han, F.-P.; Dai, Q.-H. Application of the SCS-CN Model to Runoff Estimation in a Small Watershed with High Spatial Heterogeneity. *Pedosphere* **2011**, *21*, 738–749. [[CrossRef](#)]
33. Zhang, S.; Pan, B. An urban storm-inundation simulation method based on GIS. *J. Hydrol.* **2014**, *517*, 260–268. [[CrossRef](#)]
34. Hou, J.; Du, Y. Spatial simulation of rainstorm waterlogging based on a water accumulation diffusion algorithm. *Geomat. Nat. Hazards Risk* **2020**, *11*, 71–87. [[CrossRef](#)]
35. Sun, S.; Zhai, J.; Li, Y.; Huang, D.; Wang, G. Urban waterlogging risk assessment in well-developed region of Eastern China. *Phys. Chem. Earth Parts A B C* **2020**, *115*, 102824. [[CrossRef](#)]
36. Roy, S.; Bose, A.; Singha, N.; Basak, D.; Chowdhury, I.R. Urban waterlogging risk as an undervalued environmental challenge: An Integrated MCDA-GIS based modeling approach. *Environ. Chall.* **2021**, *4*, 100194. [[CrossRef](#)]
37. Valis, D.; Hasilová, K.; Forbelská, M.; Pietrucha-Urbanik, K. Modelling Water Distribution Network Failures and Deterioration. In Proceedings of the 2017 IEEE International Conference on Industrial Engineering and Engineering Management (IEEM), Singapore, 10–13 December 2017; pp. 924–928.

38. Liu, F.; Liu, X.; Xu, T.; Yang, G.; Zhao, Y. Driving Factors and Risk Assessment of Rainstorm Waterlogging in Urban Agglomeration Areas: A Case Study of the Guangdong-Hong Kong-Macao Greater Bay Area, China. *Water* **2021**, *13*, 770. [[CrossRef](#)]
39. Pandey, A.C.; Singh, S.K.; Nathawat, M.S. Waterlogging and flood hazards vulnerability and risk assessment in Indo Gangetic plain. *Nat. Hazards* **2010**, *55*, 273–289. [[CrossRef](#)]
40. Vališ, D.; Hasilová, K.; Forbelská, M.; Vintr, Z. Reliability modelling and analysis of water distribution network based on backpropagation recursive processes with real field data. *Measurement* **2020**, *149*, 107026. [[CrossRef](#)]
41. Xu, H.; Ma, C.; Lian, J.; Xu, K.; Chaima, E. Urban flooding risk assessment based on an integrated k-means cluster algorithm and improved entropy weight method in the region of Haikou, China. *J. Hydrol.* **2018**, *563*, 975–986. [[CrossRef](#)]
42. Chattaraj, D.; Paul, B.; Sarkar, S. Integrated Multi-parametric Analytic Hierarchy Process (AHP) and Geographic Information System (GIS) based Spatial modelling for Flood and Water logging Susceptibility Mapping: A case study of English Bazar Municipality of Malda, West Bengal, India. *Nat. Hazards Earth Syst. Sci. Discuss.* **2021**, *2021*, 1–20.
43. Lin, K.; Chen, H.; Xu, C.-Y.; Yan, P.; Lan, T.; Liu, Z.; Dong, C. Assessment of flash flood risk based on improved analytic hierarchy process method and integrated maximum likelihood clustering algorithm. *J. Hydrol.* **2020**, *584*, 124696. [[CrossRef](#)]